Investigation of a Rotor- Bearing System with Bearing Clearances and Hertz Contact by Using a Harmonic Balance Method

Cristiano V. S. Villa
cristiano_viana@hotmail.com
Universidade de Brasília
Faculdade Tecnologia, Dept. Eng. Mecânica
70910-900 Brasília, DF. Brazil

Jean-Jacques Sinou
jean-jacques.sinou@ec-lyon.fr

Fabrice Thouverez
fabrice.thouverez@ec-lyon.fr
École Centrale de Lyon
Lab. de Tribologie et Dynamique dês Systèmes
69134 Ecully Cedex, France

This work is about the steady state vibration of a rotor bearing system. The rolling bearings are modeled as two degrees of freedom elements where the kinematics of the rolling elements is considered, so are the internal clearance and the Hertz contact nonlinearity. The steady state solution of the system is achieved by the harmonic balance method, validated by a numerical integration using a three-point-centered finite difference scheme. The number of harmonics employed in the harmonic balance method is examined to find the satisfactory quantity of harmonics that can describe the system dynamics. The contact regimes in the rolling elements are also explored.
Keywords*: rolling bearings, harmonic balance method, bearing clearance, Hertz contact*

Introduction

Rolling elements bearings are mechanical parts whose role is to support and locate shafts and rotating parts in machines (Avalone and Baumeister, 1999). A rolling element bearing contains two rings and between these rings, rolling elements. They allow the relative motion between the rings and also the correct positioning of them. Generally, there also exists a cage whose main function is to keep the adequate angular separation of the rolling elements.

The rolling element bearing is a complex mechanical unit. There are several studies on its mechanical behavior like the standard reference on the field, Harris (2001). Rolling elements bearings are widely used as boundary conditions for rotordynamics studies. Lim and Singh (1990) present a theory of developing a stiffness matrix that accounts for the radial displacement and bending of the shaft, including the bearing clearance and the Hertz contact between the rings and the rolling elements.

Tiwari et al. (2000) studied the influence of the bearing clearance on the dynamics of a horizontal rigid rotor, showing that this parameter is very important as it controls the regions of unstable regime and chaotic behavior. The studies were made with the harmonic balance method and the numerical integration.

Another important aspect in the bearing induced vibrations is the race waviness. Harsha et al. (2003) studied a rotor bearing system perfectly balanced considering a deep groove ball bearing with radial clearance, Hertz contact and the race waviness. The race waviness is characterized by a sinusoidal profile and produces vibration at the profile's frequency. They found that the system could present quasiperiodic, periodic and chaotic responses as well as stable and unstable regimes. The numerical investigations were made by using direct integrations.

In this paper a study of a rotor bearing system considering a stator is presented. The bearing has two in-plane degrees of freedom, considering the effects of variable stiffness, Hertz contact and radial clearance. The interaction between the weight of the rotor and the centrifugal force is of particular interest, because under this regime the rolling bearing can exhibit a very complex behavior. The method of solution is the harmonic balance method associated with the AFT (Alternating Frequency Time) strategy and the numerical integration for validation of the results.

Paper accepted November, 2006. Technical Editor: Atila P. Silva Freire.

Nomenclature

A = Sine Fourier coefficients vector
B = Cosine Fourier coefficients vector
C = Cosine Fourier coefficients vector
c = damping coefficient, Ns/m
D = damping matrix
d = distance, m
F = force vector
F = bearing force, N
K = stiffness matrix
k = stiffness, N/m
k_H = bearing ball stiffness, N/m$^{3/2}$
N_b = number of balls of the rolling bearing
M = mass matrix
m = mass, kg
R = inner groove radius of the bearing, m
R_b = radius of a bearing ball, m
S = Sine Fourier coefficients vector
s = curvilinear abscissa
t = time, s
X = displacement vector
x = horizontal displacement, m
Y = Displacement vector in the frequency domain
y = vertical displacement, m
Z = Force vector in the frequency domain

Greek Letters

δ = relative radial displacement
Ω = spin speed of the rotor, rad/s
θ_i = angular position of the ith ball, rad
$\int\theta$ = angular spacing between two bearing balls, rad

Subscripts

k = harmonic number
r = relative to rotor
s = relative to stator
u = relative to unbalance
x = x direction
y = y direction

Superscripts

p = step in the curvilinear abscissa
R = relative to resultant
t = transpose

Equations of Motion

The analyzed system is a horizontal Jeffcott rotor connected to a flexible stator by a rolling element bearing installed at its midspan. The bearing is modeled as a two-degree-freedom element with radial clearance and Hertz contact between the races and the rolling elements. The friction in the bearing is assumed to be zero. The excitation due to the bearing is assumed to be small in comparison to the unbalance forces and then will not be considered.

The variable stiffness of the rolling bearing is modeled based on the internal kinematics of the rolling elements. Figure 1 shows a rolling element bearing with its fixed frame of reference and the spin direction of the rotor. The bearing has N_b rolling elements and each rolling element has an angular position θ_i. The cage keeps the angular spacing of the rolling elements constant, so the angular space between 2 balls is equal to $\Delta\theta = 2\pi/N_b$.

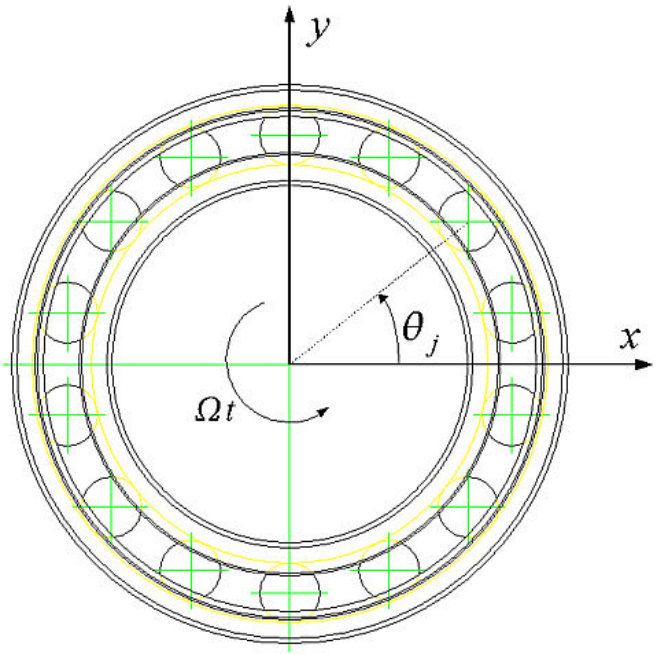

Figure 1. Rolling element position in the bearing.

Considering a ball bearing, the angular positions θ_i, $1 \le i \le N_b$, are functions of the spin speed of the rotor, the radius of the ball and the radius of the inner ring, as shown by the following equation:

$$\theta_i = \frac{\Omega}{2}\left(1 - \frac{R_b}{R_b + R}\right)t + 2\pi\frac{(i-1)}{N_b} \tag{1}$$

where R_i is the inner groove radius and R_b is the ball radius. Knowing the position of the rolling elements, the restoring force can be calculated by making the hypothesis that the contact between the rolling element and the races is Hertz contact. At first the relative displacement between the inner and the outer ring must be determined at each rolling element:

$$\delta_i = (x_r - x_s)\cos(\theta_i) + (y_r - y_s)\sin(\theta_i) \tag{2}$$

Then, the restoring force is calculated for each rolling element:

$$Q_i = \begin{cases} k_H(\delta_i - \delta)^{3/2} & , \ \delta_i > \delta \\ 0 & , \ \delta_i \le \delta \end{cases} \tag{3}$$

The forces acting on the rotor by the rolling element bearing the x and y directions are:

$$\begin{bmatrix} F_x^R \\ F_y^R \end{bmatrix}(\mathbf{X}) = -\sum_{i=1}^{N_b} Q_i \begin{bmatrix} \cos(\theta_i) \\ \sin(\theta_i) \end{bmatrix} \tag{4}$$

Finally, the equations of motion for the rotor bearing system with a nonlinear rolling element bearing and a stator are:

$$\begin{aligned} &m_s\ddot{x}_s + c_s\dot{x}_s + k_s x_s = F_x^R \\ &m_s\ddot{y}_s + c_s\dot{y}_s + k_s y_s = F_y^R - m_s g \\ &m_r\ddot{x}_r + c_r\dot{x}_r + k_r x_r = -F_x^R + m_u d_u \Omega^2 \cos(\Omega t) \\ &m_r\ddot{y}_r + c_r\dot{y}_r + k_r y_r = -F_y^R + m_u d_u \Omega^2 \sin(\Omega t) - m_r g \end{aligned} \tag{5}$$

It can be seem from Equation (5) that the stator dynamics is coupled with the rotor dynamics by the nonlinear forces of the rolling element bearing.

Harmonic Solutions

The method for searching the harmonic solutions of the equations (5) is the harmonic balance method with the alternating frequency time strategy (HBM AFT). In this method a harmonic solution for the system of nonlinear differential equations is assumed, transforming this system in a nonlinear algebraic system on equations. The nonlinearities are evaluated in the time domain and the harmonic solution is evaluated in the frequency domain.

The equations of motion are written in the following form:

$$\mathbf{M}\ddot{\mathbf{X}} + \mathbf{D}\dot{\mathbf{X}} + \mathbf{K}\mathbf{X} = \mathbf{F_0} + \mathbf{F_u} + \mathbf{F_R}(\mathbf{X}) = \mathbf{F} \tag{6}$$

In the Equation (6), **X** is the vector of displacements, **M** is the constant mass matrix, **K** is the stiffness matrix and **D** is the damping matrix. The vector **F** contains the weight, the unbalance and the bearing forces:

$$\mathbf{F} = \begin{bmatrix} 0 \\ -m_s g \\ 0 \\ -m_r g \end{bmatrix} + \begin{bmatrix} 0 \\ 0 \\ m_u d_u \Omega^2 \cos(\Omega t) \\ m_u d_u \Omega^2 \sin(\Omega t) \end{bmatrix} + \begin{bmatrix} F_x^R \\ F_y^R \\ -F_x^R \\ -F_y^R \end{bmatrix}(\mathbf{X}) \tag{7}$$

The response of the system is assumed to have only integer multiples of the exciting frequency, assuming the truncated Fourier series form:

$$\mathbf{X}(t) = \mathbf{B}_0 + \sum_{j=1}^{N}\left(\mathbf{A}_j \sin(j\Omega t) + \mathbf{B}_j \cos(j\Omega t)\right) \tag{8}$$

The excitation forces are also demonstrated by a sum of harmonics:

$$\mathbf{F}(t) = \mathbf{C}_0 + \sum_{j=1}^{N}\left(\mathbf{S}_j \sin(j\Omega t) + \mathbf{C}_j \cos(j\Omega t)\right) \tag{9}$$

The equations (8) and (9) are inserted in the equation of motion (6) and the nonlinear system of equations become a system of nonlinear algebraic equations:

$$\begin{bmatrix} \mathbf{K} & & & & \\ & \ddots & & & \\ & & \mathbf{\Lambda}_k & & \\ & & & \ddots & \\ & & & & \mathbf{\Lambda}_N \end{bmatrix} \begin{bmatrix} \mathbf{B}_0 \\ \vdots \\ \mathbf{Y}_k \\ \vdots \\ \mathbf{Y}_N \end{bmatrix} = \begin{bmatrix} \mathbf{C}_0 \\ \vdots \\ \mathbf{Z}_k \\ \vdots \\ \mathbf{Z}_N \end{bmatrix} \tag{10}$$

The fist block of equations accounts for the static deformation. The block $\mathbf{\Lambda}_k$ is a dynamical stiffness of the k^{th} harmonic given by:

$$\mathbf{\Lambda}_k = \begin{bmatrix} \mathbf{K} - \mathbf{M}(k\Omega)^2 & -\mathbf{D}(k\Omega) \\ \mathbf{D}(k\Omega) & \mathbf{K} - \mathbf{M}(k\Omega)^2 \end{bmatrix} \tag{11}$$

The vector $\mathbf{Y_k}$ is a vector containing the unknown Fourier coefficients and $\mathbf{Z_k}$ is the vector of the Fourier coefficients of the excitation:

$$\mathbf{Y}_k = \begin{bmatrix} \mathbf{A}_k \\ \mathbf{B}_k \end{bmatrix} \quad ; \quad \mathbf{Z}_k = \begin{bmatrix} \mathbf{S}_k \\ \mathbf{C}_k \end{bmatrix}$$

The equation (10) can be written as:

$$\mathbf{H}(\mathbf{Y},\Omega) = \mathbf{\Lambda Y} - \mathbf{Z}(\mathbf{Y}) \tag{13}$$

To solve this equation it is needed to have the Fourier series coefficients of the nonlinear forces, a task that can be difficult to handle analytically by using the mathematical definition of the coefficients.

Another approach to get the coefficients is the AFT strategy (Cameron and Griffin, 1989). With the Fourier series coefficients of the **Y** vector, the solution **X** can be evaluated by using the Equation (8). Then the excitation forces, including the nonlinear forces, can be calculated by using the Equation (7). The Fourier series coefficients are found by the numerical evaluation of the following integrals (Weisstein, 2004):

$$\begin{aligned} \mathbf{C}_0 &= \frac{2}{T}\int_0^T \mathbf{F}(t)\,dt \\ \mathbf{C}_i &= \frac{2}{T}\int_0^T \mathbf{F}(t)\cos(i\Omega t)\,dt \\ \mathbf{S}_i &= \frac{2}{T}\int_0^T \mathbf{F}(t)\sin(i\Omega t)\,dt \end{aligned} \tag{14}$$

Finally the equation (13) is solved by using a nonlinear system of equations solver like the Broyden method (Broyden, 1965). A special implementation of the Broyden method was developed containing an arc-length continuation scheme (Nayfeh and Balachandran, 1995), where the spin speed Ω is regarded as a new unknown of the system, and the control variable is now the arc-length of the hypercurve described by the tip of the vector $(s,[\mathbf{Y};\Omega])$. The curvilinear abscissa s must obey the arc-length equation:

$$\left(s - {}^{(p-1)}s\right)^2 = \left(\mathbf{Y} - {}^{(p-1)}\mathbf{Y}\right)^t \left(\mathbf{Y} - {}^{(p-1)}\mathbf{Y}\right) + \left(\Omega - {}^{(p-1)}\Omega\right)^2 \tag{15}$$

where ${}^{(p-1)}s$, ${}^{(p-1)}\boldsymbol{Y}$ and ${}^{(p-1)}\Omega$ are respectively the curvilinear abscissa of the previous step, the Fourier coefficients vector of the previous step and the spin speed found in the previous step.

The efficacy of this strategy is highly influenced by the predictor employed. The simulations presented here use a 3th degree Lagrange polynomial predictor based on the previous solutions and the corresponding curvilinear abscissas. The step over the curvilinear abscissa is controlled by the normalized dot product of the last two good solutions. If the dot product is superior to 0.9, the steps are increased by a 1.02 factor, else the increment is divided by 2. These values are empirical.

Results of the Simulations

The system under study has the following characteristics: $m_s = 30\,\text{kg}$, $m_r = 50\,\text{kg}$, $\omega_{0r} = 141.42$ rad/s, $\omega_{0s} = 577.35$ rad/s, $\zeta_r = 0.02$ and $\zeta_s = 0.05$. The rolling bearing has 16 balls each with radius of 10 mm and the bore diameter is equal to 100 mm. The stiffness of each ball is 2×10^{10} N/m$^{3/2}$, a value compatible with the results of a rolling element stiffness calculation following the methodology presented by Harris (2001). The bearing clearance is equal to 20μm and the unbalance (0.2) is chosen to study the contact phenomena not so near the resonance peak.

At first the response of the system is calculated for a growing spin speed from 0 to 70 Hz with 5 harmonics to show a global response curve for the X direction, as showed in the Figure 2.

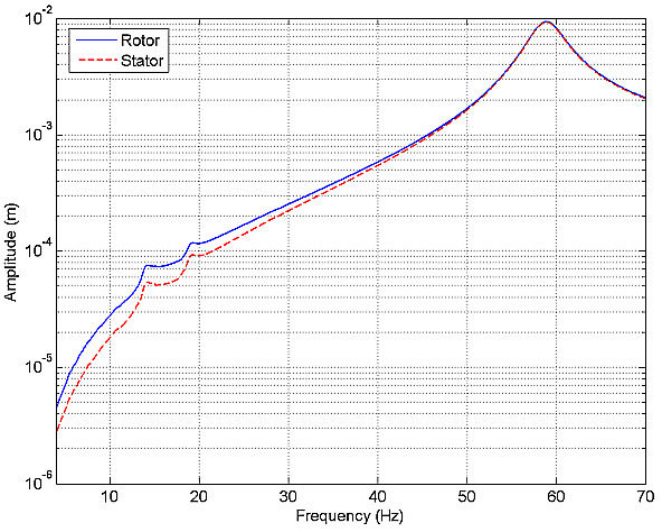

Figure 2. X direction response of the rotor and the stator.

The region of interest is that between 10 Hz and 23 Hz. To see the dynamics of the rotor-stator in this frequency range, a plot of the evolution of the orbits in function of the frequency of rotation is shown in the Figure 3. It can be seen that the orbit near 10 Hz is very near an elliptical orbit. When the frequency of rotation is between 11 Hz and 16 Hz, the orbits start to have a complex morphology, forming even star shaped orbits and hexagon shaped orbits. Between 16 Hz and 20 Hz, the orbits are less complex than those found for the range 11 Hz – 16 Hz, having basically 2 lobes. After 20 Hz, the orbits recover the elliptical form.

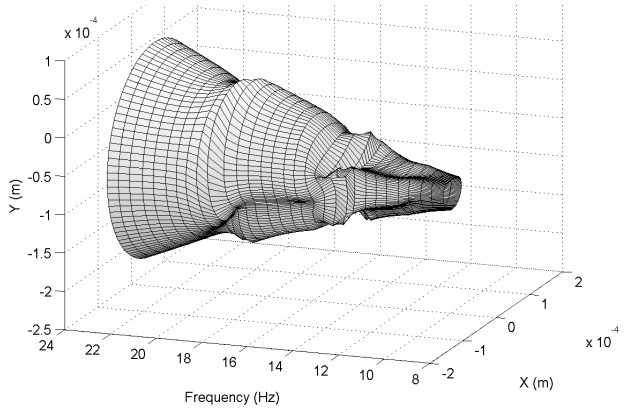

Figure 3. Evolution of the orbits from 10 Hz to 23 Hz.

To verify the quality of the results given by the HBM AFT method, a comparison of its results (keeping 10 harmonics) with these by direct integration is performed. The system of equations (5) is integrated by using a centered finite difference scheme (Géradin and Rixen, 1997) with 3000 discretisations points over the time and 1500 periods of integration for Ω between 5 Hz and 20 Hz. The comparison shows a good accordance between the results obtained by the two methods, as the figure 4 illustrates.

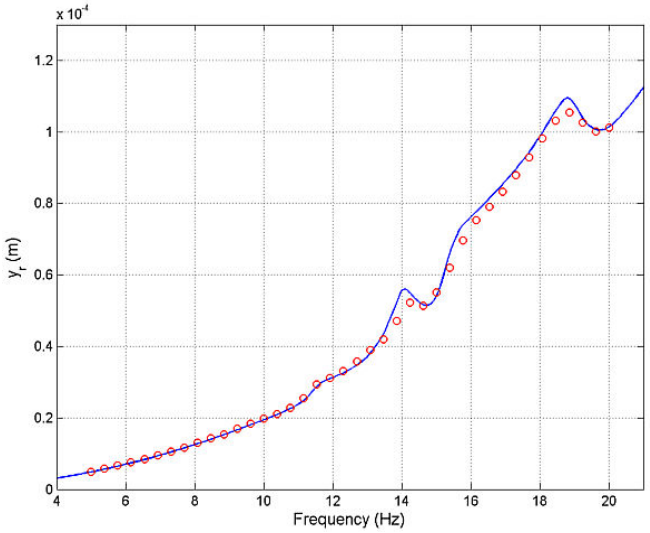

Figure 4. HBM AFT (—) results against the direct integration results (O).

For a deeper comparison between the two methods, the orbits are analyzed. The first case considers the rotor at 10.4 Hz and the orbits are shown in the Figure (5). The figure shows the orbit of the stator at a near elliptical form and shows that the rotor does an orbit with the top and the upper right and upper left in a flattened fashion. The HBM AFT and direct integration solutions are very well correlated.

At 12.7 Hz (Figure (6)), the stator orbit has a hexagonal form while the rotor has a pentagonal orbit. Again the HBM AFT and the direct integration give almost the same results. At 14.2 Hz (Figure (7)) the system has the most complex orbits. The rotor and the stator have the orbits in a star-shaped form with a loop at the lower left tip. The accordance between the two methods is not as good as it is for the two previous cases.

Finally, at 19.2 Hz (Figure (8)), the rotor and the stator are running in a two-lobe orbit and the two methods of solution in accordance with each other. For the frequencies above 19.2 Hz the accordance between the two methods is always good.

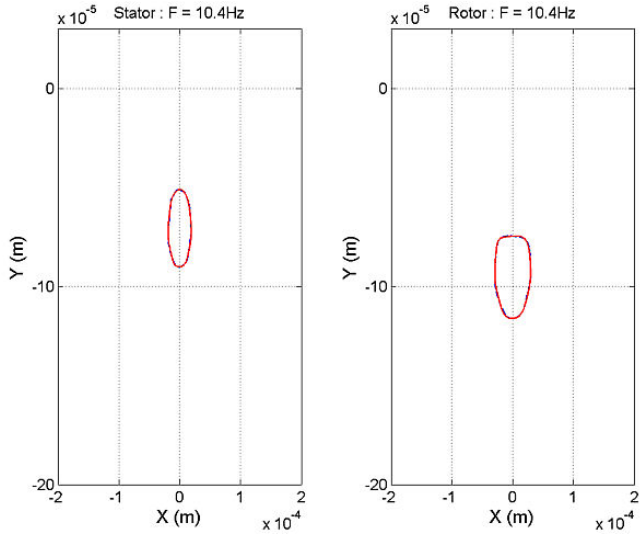

Figure 5. HBM AFT with 10 harmonics (—) and direct integration (– – –).

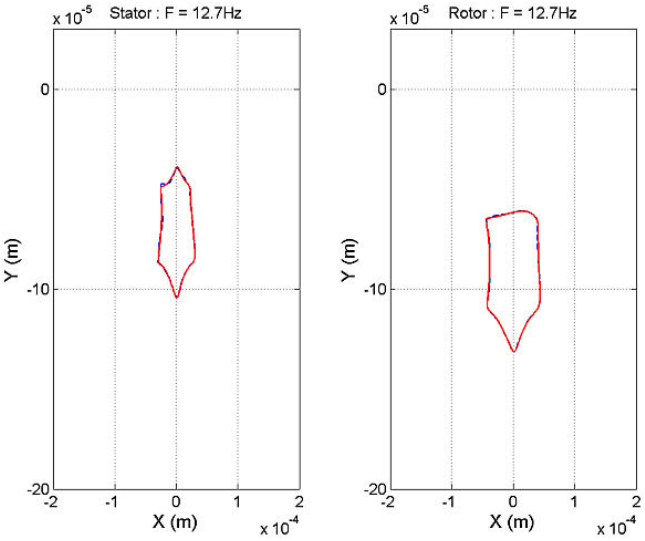

Figure 6. HBM AFT with 10 harmonics (—) and direct integration (– – –).

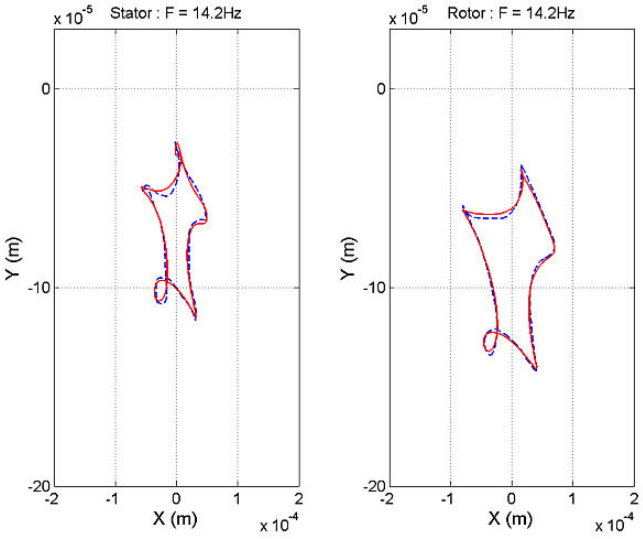

Figure 7. HBM AFT with 10 harmonics (—) and direct integration (– – –).

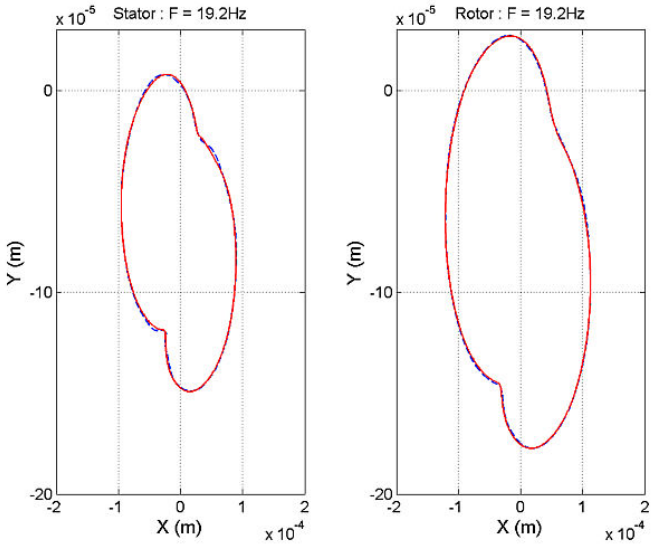

Figure 8. HBM AFT with 10 harmonics (—) and direct integration (– – –).

These validation results were produced with a 10 harmonics HBM AFT method. However, this quantity of harmonics needs a reasonably high computational effort and may not be necessary for all the frequency range, only for the complex regimes as shown in figure 9. This figure shows a comparison of the HBM AFT method with the direct integration method at 14.2 Hz, but this time the number of harmonics kept in the solution is varied to verify how good the HBM AFT estimation can be.

In this case, as the direct integration solution is known, a spectral analysis could reveal the number of harmonics needed to get a good HBM approximation. But assuming that the solution is unknown (as it is in most cases), the figure shows how the increase in number of harmonics makes the HBM AFT approach to the direct integration solution. The same comparison is made for the rotor at 19.2 Hz (Figure 10), showing that the direct integration solution can be well mimetized by the 3 harmonics HBM AFT solution.

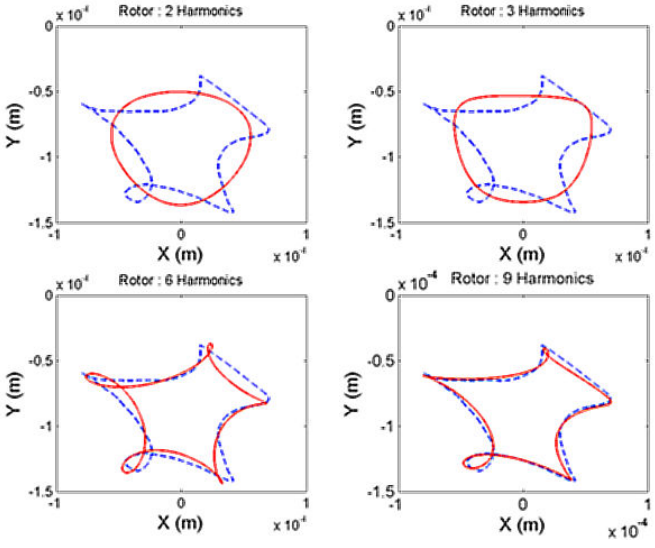

Figure 9. HBM AFT (—) and direct integration (– – –).

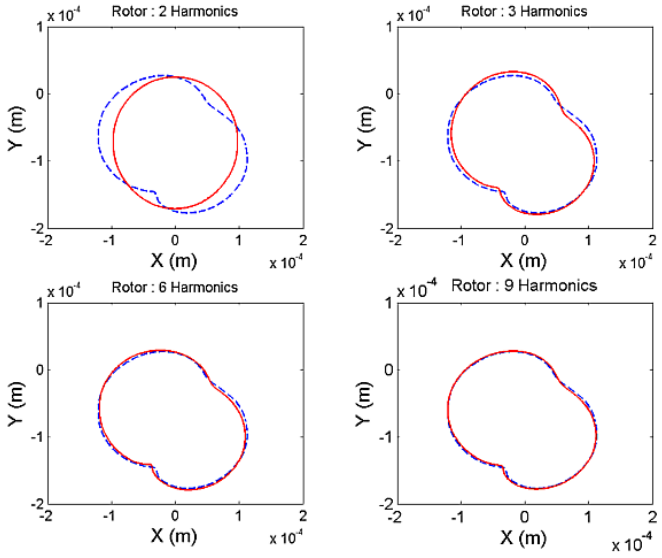

Figure 10. HBM AFT (—) and direct integration (– – –).

The HBM AFT solution can also show how the rolling elements of the bearing act. For example, in a period of revolution, how many rolling elements are in contact with the outer ring? To answer this question, one tactic is to create a function per rolling element that is zero valued over all the period of revolution of the bearing cage except the instants of contact. When the function is evaluated for all rolling elements and put in graphical form, the contact behavior of the bearing can be understood. In the following discussion, the number of harmonics kept in the solution for the following analysis is equal to 10, and the time is discretized over one period of revolution of the bearing cage.

Starting with Ω=5 Hz (Figure 11), the graphic shows that all the rolling elements are taking part in the motion of the rotor. It can be easier to see if one takes a closer look at one of the rolling elements. For this particular ball, the horizontal line indicates the fraction of the period of revolution of the bearing cage where the contact exists. The same idea holds for the rest of the balls. Then, the Figure 11 shows that the contact time per ball is not so different from one ball to the other, that is, the shaft is whirling almost homogenously at the bottom of the bearing, as the contact goes from the ball 16 to the ball 1 and considering the direction of rotation of the shaft. This graphic can also show how many balls are in contact with the outer ring. Choosing any instant inside the considered time interval, and tracing a vertical line at this instant, one can see that there are at least 3 rolling elements in contact with the outer ring.

At Ω=10.4 Hz, Figure 12 shows that the contacts now are happening in a more pronounced way in two zones: from the ball 6 until the ball 9 and from the ball 15 to the ball 2. Also the rotor is still moving at the bottom of the bearing.

At 15 Hz, the figure 13 shows there are two zones of the bearing without contact: from the balls 10 to 13 and from the balls 3 to 5. There are two contact zones from the ball 14 to the ball 2 and from the ball 6 to the ball 9 and these two zones are in opposite sides of the bearing. The contact and noncontact zones are arising because of the participation of the bearing clearance in the dynamics of the system.

When the rotational frequency reaches 19.2 Hz (Figure 14), the noncontact zones are already gone, but there are two zones where the contact time is longer. At this frequency the orbit is almost elliptical and the shaft travels over the outer ring of the bearing since the bearing clearance is consumed. The order of contact for

the balls is inversed compared with the Figure 12 because of the motion of the rotor.

The last case shows the bearing contacts for the system at 35 Hz (Figure 15), where all the rolling elements are engaging in almost the same contact time over the period of rotation.

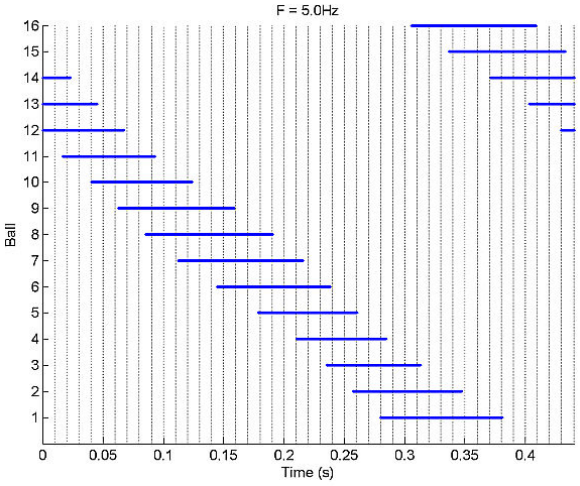

Figure 11. Contact time for each ball (F=5.0 Hz).

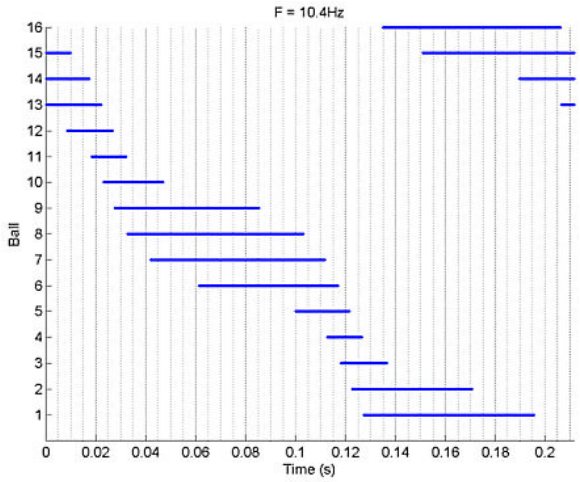

Figure 12. Contact time for each ball (F=10.4 Hz).

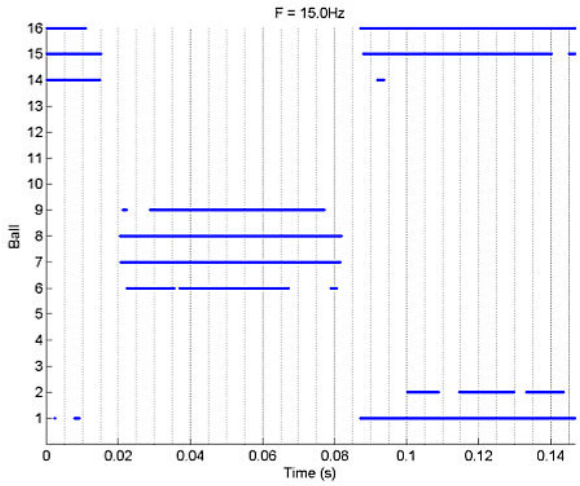

Figure 13. Contact time for each ball (F=15.0 Hz).

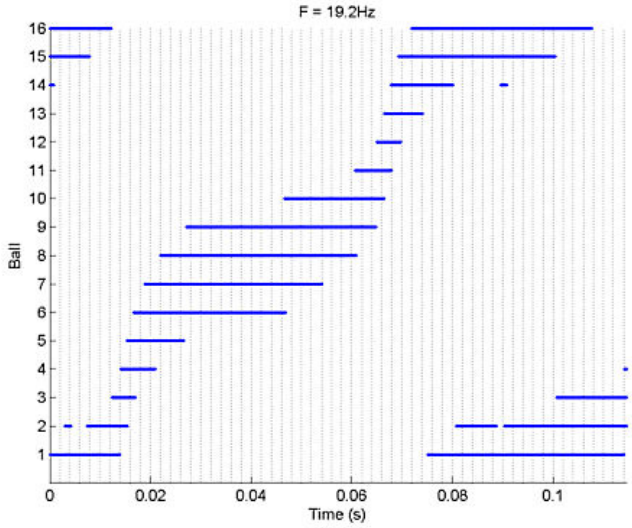

Figure 14. Contact time for each ball (F=19.2 Hz).

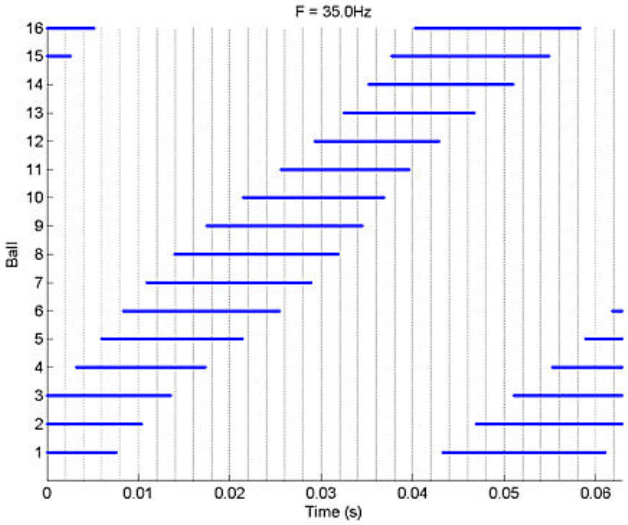

Figure 15. Contact time for each ball (F=35.0 Hz).

Conclusions

This work presented one implementation of the harmonic balance method coupled with the AFT strategy, where the nonlinearities are evaluated in the time domain and the response of the system is calculated in the frequency domain. The system under study is a Jeffcott rotor connected to a stator through a ball bearing at the midspan.

The results of the HBM AFT technique are compared with a direct integration solution over the range of rotation frequencies of interest, and this comparison showed that the HBM AFT tends to give the same results as those of the direct integration.

It was found that there is a frequency range (12 - 20 Hz) where the behavior of the system is complex because of the iteration of the unbalance forces and the weight of the rotor, considering the bearing clearance. The motion of the rotor, in this frequency range, changes from one taking place at the bottom of the bearing to the other where the shaft travels over the outer ring of the bearing. Between these two regimes, there are situations where not all the balls of the bearing are touching the outer ring.

Acknowledgment

The authors thank CAPES/MEC (Coordenação de Aperfeiçoamento de Pessoal de Nível Superior do Ministério da Educação - Brazil) for the support given to this research.

Bibliography

Avallone, E. A., Baumeister, T., 1999, “Marks’ Standard Handbook for Mechanical Engineers”, McGraw Hill.

Broyden, C. G., 1965, "A Class of Methods for Solving Nonlinear Simultaneous Equations." Mathematics of Computations, vol. 19, 577-593.

Cameron, T. M., Griffin, J. H., 1989, “An Alternating Frequency/Time Domain Method for Calculating the Steady State Response of Nonlinear Dynamic Systems”, Journal of Applied Mechanics, Vol. 56, pp. 149-154.

Eric W. Weisstein, 2004, "Fourier Series." From MathWorld--A Wolfram Web Resource. http://mathworld.wolfram.com/FourierSeries.html.

Géradin, M., Rixen, D., 1997, “Théorie des Vibrations – Application à la Dynamique des Structures”, 2ème édition, Masson.

Harris, T. A., 2001, “Rolling Bearing Analysis”, John Wiley and Sons, 4th edition.

Harsha, S. P., Sandeep, K., Prakash, R., 2003, The Effect of Balanced Rotor on Nonlinear Vibrations Associated with Ball Bearings, International Journal of Mechanical Sciences, Vol. 45, pp. 725-740.

Lim, T. C., Singh, R., 1990, “Vibration Transmission Through Rolling Elements Bearings, Part I: Bearing Stiffness Formulation”, Journal of Sound and Vibration, Vol. 139, No. 2.

Nayfeh, A. H., Balachandran, B., 1995, Applied Nonlinear Dynamics: Analytical, Computational and Experimental Methods, Wiley, New York.

Tiwari, M., Gupta, K., Prakash, O., 2000, “Effect of Radial Clearance of a Ball Bearing on the Dynamics of a Balanced Horizontal Rotor”, Journal of Sound and Vibration, Vol. 238, No.5, pp. 723-756.0